EJSO 2003; **29**: 867–878
doi:10.1016/j.ejso.2003.09.012

EJSO
European Journal of Surgical Oncology

Size and geometry of hepatic radiofrequency lesions

S. Mulier*, Y. Ni†, Y. Miao‡, A. Rosière*, A. Khoury*, G. Marchal† and L. Michel*

*Department of Surgery, University Hospital of Mont-Godinne, Catholic University of Louvain, Yvoir, Belgium; †Department of Radiology, University Hospital Gasthuisberg, Catholic University of Leuven, Leuven, Belgium; and ‡Department of General Surgery, The First Affiliated Hospital of Nanjing Medical University, Nanjing, People's Republic of China

Aim: To report and compare the size and geometry of hepatic radiofrequency (RF) lesions using the currently available commercial devices.
Methods: A literature search was carried out for the period from January 1st 1990 to June 15th 2003. The commercial suppliers were asked to provide all available data. For each electrode and protocol, size and geometry of single-cycle thermal lesions were registered.
Results: No information at all on size and geometry of the inducible lesions was available for 17 of the 28 current commercial electrodes. Many descriptions of RF lesions are limited to the mean transverse diameter. With normal blood flow, diameter of lesions is often smaller than suggested by the length of the electrode tip or the diameter of the deployed prongs. Lesions are rarely perfect spheres but either ellipses or flattened spheres. Distortion of the RF lesion by nearby blood vessels is very common. Fusion of thermal zones between prongs of expandable electrodes can be incomplete. Blood flow interruption using a Pringle maneuver yields larger lesions that are less distorted and more complete.
Conclusions: There is insufficient experimental data for many electrodes that are currently used in patients. RF companies should provide these data before releasing electrodes for use. For those electrodes for which data exist, coagulation lesions are often smaller, less spherical, less complete and less regular than generally presumed. Accurate knowledge of size and geometry of RF lesions is crucial to prevent local recurrence.

Key words: radiofrequency; neoplasm; liver.

INTRODUCTION

Radiofrequency (RF) coagulation of inoperable liver tumours is a valuable technique. By December 2001, at least 3670 cases had been reported.[1] The local recurrence rate varies among series but may be as high as 60% after 6 months.[2] Real-time monitoring of the area of coagulation with ultrasound is unreliable.[3–6] Therefore, radiofrequency needs to be carried out based on size and geometry obtained in animal experiments or in clinical studies. A systematical description of these data, however, was not available up till now. Overestimation of expected coagulation size and an unrealistic image of a perfect spherical geometry may contribute to failure of local tumour control.

Correspondence to: Dr S. Mulier, MD, Department of Surgery, University Hospital of Mont-Godinne, Catholic University of Louvain, Avenue du Dr. Thérasse 1, Yvoir B-5530, Belgium. Tel.: +32-81-42-30-51; Fax: +32-81-42-20-07; E-mail: stefaan.mulier@mont.ucl.ac.be

MATERIALS AND METHODS

We carried out a search of Current Contents, Medline and PubMed for the period from January 1st 1990 to June 15th 2003 using the keywords radiofrequency, radio-frequency or radio frequency and liver or hepatic or hepatocellular in all languages except Japanese and Chinese. All abstract supplements from the same period published in Radiology, American Journal of Radiology, Journal of Vascular and Interventional Radiology, European Radiology, and Surgical Endoscopy were searched manually. Relevant papers were also identified from the reference lists of the papers previously obtained through the search and from abstracts from recent international meetings. The five companies that produce commercial RF electrodes, Radionics®, RITA® Medical Systems, Radiotherapeutics®, Berchtold®, and Invatec® were contacted and asked to provide the most recent data on technical performance of their electrodes.

0748–7983/$30.00

Study models

We only selected papers which included observations *in vivo* in pig liver and in patients. Experiments *ex vivo* and experiments in small animals (rabbits, rats) were excluded. Only measurements obtained by macroscopic or microscopic analysis (hematoxylin and eosin, or, preferably, mitochondrial enzyme stains); or by CT/MRI with contrast injection, were included. Only observations with electrodes that were for sale at the time of writing (Table 1, Fig. 1) were included.

Definitions (Fig. 2)

All measurements exclude the hyperaemic histological or radiological rim.

radius is defined as the distance between the electrode shaft and the edge of the coagulation lesion, perpendicular to the electrode shaft, at the equator of the RF lesion (Fig. 2(A)).

tranverse diameter is defined as the distance between two opposite edges of the coagulation lesion, perpendicular to the electrode shaft, at the equator of the RF lesion (Fig. 2(B)).

length is defined as the distance between the proximal and the distal edge of the coagulation lesion, in the axis of the electrode (Fig. 2(C)).

ellipticity quantitatively describes the lesion shape in the axial plane and is calculated as the ratio between length and transverse diameter: this way, a ratio of 1.0 corresponds to a spherical lesion; a ratio $>$ 1.0 to an elliptical lesion; and a ratio $<$ 1.0 to a flattened sphere (Fig. 2(D)).

distortion refers to the percentage of RF lesions that are distorted, i.e. asymmetrically smaller (type 1) or larger (type 2) than expected (Fig. 2(E)).

completeness of fusion describes the RF lesion in the transverse plane when multi-prong electrodes are used (Fig. 2(F)). It refers to the quality of fusion of the separate coagulation zones around each prong into

Table 1 Commercial radiofrequency electrodes

Electrode	Length tip (cm)	Diameter tip (mm)	n active prongs	Diameter expanded prongs (cm)
Radionics® Cool-tip RF®				
Single 1-cm tip	1	1.5	/	/
Single 2-cm tip	2	1.5	/	/
RITA Medical Systems®				
Model 30	/	1.8	4	3
Model 70	/	1.8	7	3
Model 75/Starburst®	/	1.8	7	3
Model 90/Starburst XL®	/	2.1	9	5
Model 100/Starburst XLi®50	/	2.1	5 (+4 neutral)	5
Model 100/Starburst XLi®70	/	2.1	5 (+4 neutral)	7
Radiotherapeutics® LeVeen®				
2-cm tip	/	1.9	8	2
3-cm tip	/	1.9	10	3
3.5-cm tip	/	1.9	10	3.5
4-cm tip	/	1.9	12	4
Berchtold® HiTT®				
1-cm tip/1.2 mm diameter	1	1.2	/	/
1.5-cm tip/1.6 mm diameter	1.5	1.6	/	/
1.5-cm tip/1.7 mm diameter	1.5	1.7	/	/
1.5-cm tip/2 mm diameter	1.5	2	/	/
2-cm tip/1.6 mm diameter	2	1.6	/	/
2-cm tip/2 mm diameter	2	2	/	/
Invatec® MIRAS®				
IOC 3-cm tip	3	6	/	/
IOC 4-cm tip	4	6	/	/
IOC 5-cm tip	5	6	/	/
LC 2.5-cm tip	2.5	2.8	/	/
LC 3-cm tip	3	2.8	/	/
LC 3.5-cm tip	3.5	2.8	/	/
LN	/	2	4	2.2
RC	/	1.1	1 coil	0.9 × 1.0

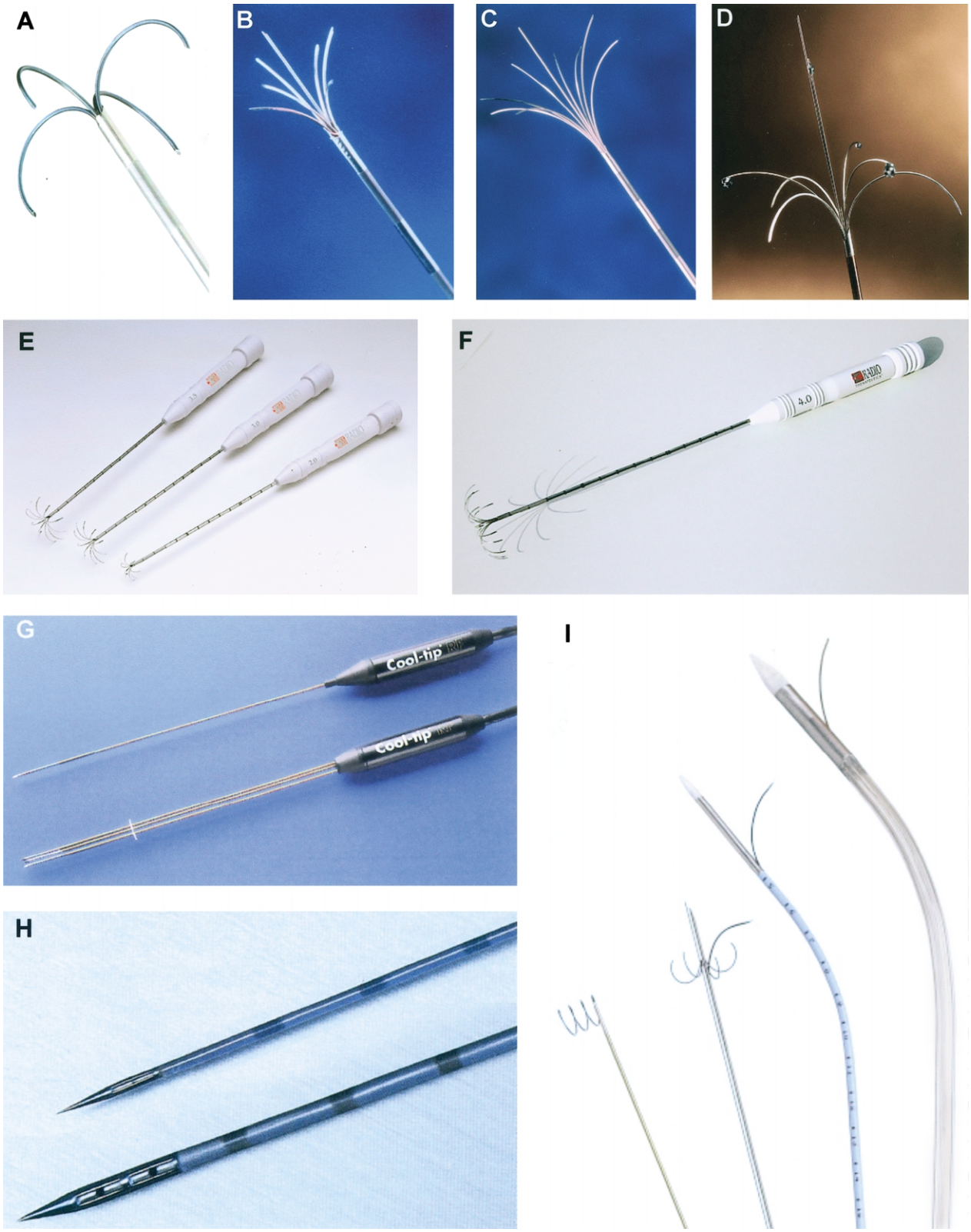

Figure 1 Commercial electrodes (a): (A) RITA® Medical Systems model 30, (B) RITA® Medical Systems model 70, (C) RITA® Medical Systems model 90/StarBurst XL®, (D) RITA® Medical Systems model 100/StarBurst XIi® 70, (E) Radiotherapeutics® LeVeen® 2-, 3- and 3.5-cm, and (F) Radiotherapeutics® LeVeen® 4-cm; (b): (G) Radionics® Cool-tip RF® single 3-cm tip and cluster, (H) Berchtold® HiTT® 1-cm tip/1.2 mm diameter and 1.5-cm tip/2 mm diameter, and (I) Convatec® MIRAS RC®, MIRAS LN®, MIRAS LC®, MIRAS IOC® (from left to right).

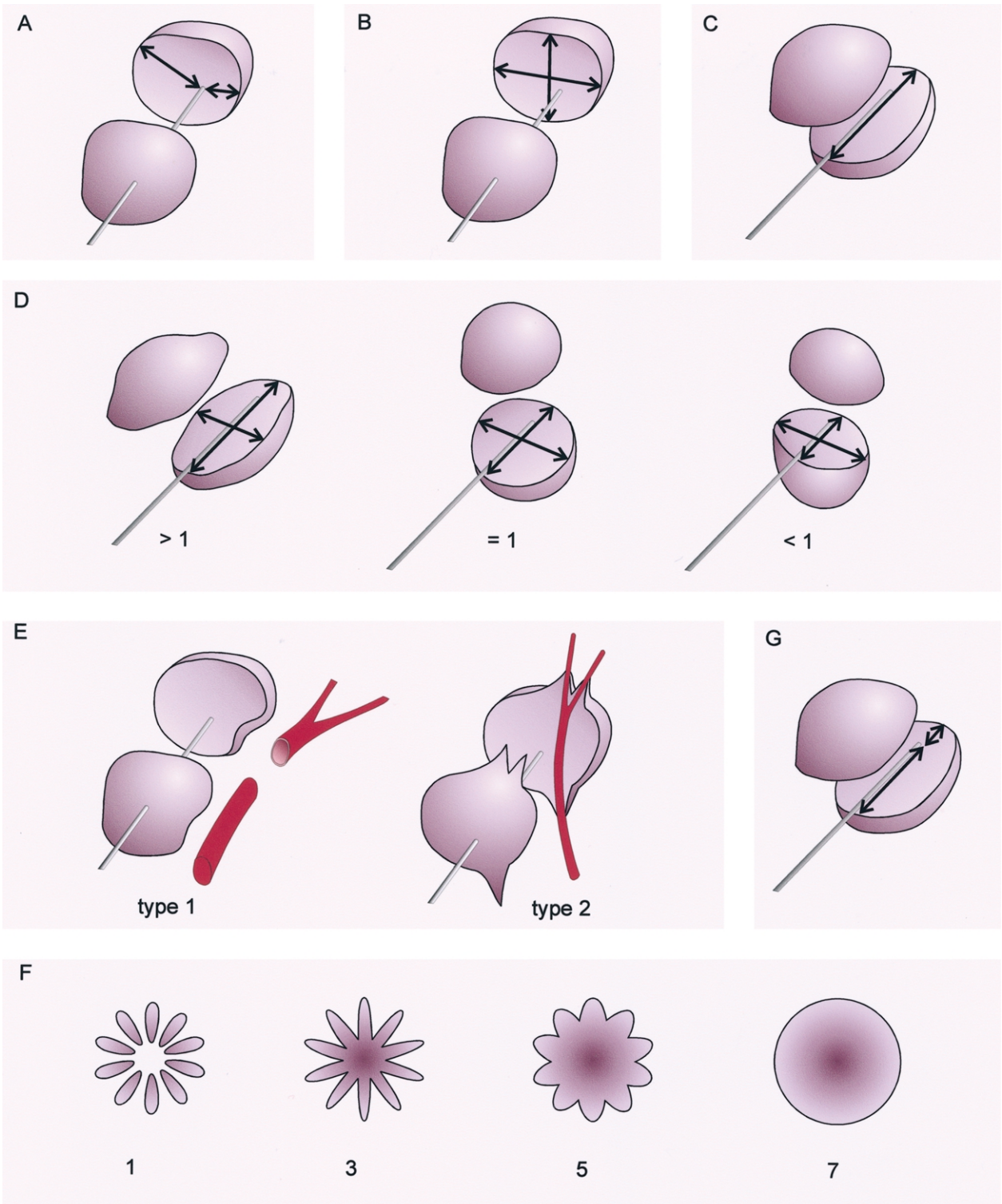

Figure 2 Definitions: (A) radius (minimal and maximal) (arrows), (B) tranverse diameter (minimal and maximal) (arrows), (C) length (arrow), (D) ellipticity index, (E) distortion type 1: lesion asymmetrically smaller than expected e.g. by cooling effect of nearby blood vessel; distortion type 2: lesion asymmetrically larger than expected e.g. by preferential diffusion of saline along vessels, (F) Chinn score of completeness of fusion, (G) relation to the electrode tip (arrows).

one spherical RF lesion. It can be quantified using the score developed by Chinn:[7] 1 refers to a discontinuous coagulation; 3 describes a central continuous zone of necrosis with peripheral deep clefts (>50% of the radius) between prongs; 5 is attributed when the peripheral clefts are shallow (<50% of diameter); 7 is the score for a perfect sphere; intermediate values refer to asymmetrical lesions that have components of 2 of the above basic shapes.

relation to the electrode tip is defined by two distances: between the proximal edge of the coagulation lesion and the electrode tip; and between the distal edge of the coagulation lesion and the electrode tip. For expandable electrodes, the prongs are not taken into account.

Description of the instruments

The *Radionics*® single or triple electrodes are cooled internally by perfusing cold saline through the electrode. They are used with a 200 W generator. Power is delivered during a fixed duration of time, either continuously or in the pulsed current mode.[8] In the latter, an automated algorithm interrupts generator output for a few seconds when impedance starts to rise.

The *RITA*® *model 30* and *model 70* electrodes are used with a 50 W generator; newer electrodes are used with a 150 W generator. The *RITA*® *model 30* electrode contains four deployable prongs, each with a thermistor at its tip. Power is increased to 50 W until the target temperature is reached, and regulated automatically to maintain this temperature for a chosen time. The *RITA*® *model 75 (StarBurst*®*)*, which has seven prongs, has a similar treatment protocol. The *RITA*® *model 90 (StarBurst XL*®*)* allows mean coagulation diameter to be varied with deployment of the prongs.[9,10] The *RITA*® *model 100 (StarBurst XLi*®*)* has five active electrodes with infusion sites for hypertonic saline at the end. They alternate with four neutral prongs with thermocouples at their tip to monitor the tissue temperature. This electrode is deployed gradually.[11] Two subtypes exist to create RF lesions of up to 5 cm or up to 7 cm.

The *Radiotherapeutics*® LeVeen® electrodes contain eight to twelve deployable prongs. The 2, 3 and 3.5 cm electrodes are used with a 100 W generator; the 4 cm electrode with a 200 W generator. Each electrode has its own protocol.[12–18] In general, the initial power is increased in small increments to a maximum power. Treatment continues for several minutes or until a precipitous drop in power output ('roll-off') occurs, as tissue impedance increases by coagulative necrosis. After a short pause, power is reapplied at a value which is a fraction lower than the maximum power until roll-off occurs again.

The *Berchtold*® HiTT® hollow electrodes have one or more holes at the tip through which an isotonic or hypertonic saline solution at room temperature is infused into the tissue during RF coagulation. A fixed power is delivered by a 60 W generator during a predetermined time, according to the desired coagulation diameter.[19]

The *Invatec*® MIRAS® electrodes all have a bent thermistor that curves away from the tip to monitor tissue temperature. They are activated by a 100 W generator. Each electrode has its own protocol.[20] The *MIRAS RC*® is a unique type electrode with a coil that leaves the tip and is deployed perpendicularly to the shaft. The *MIRAS LN*® is an expandable electrode with four prongs that are deployed by pulling rather than by pushing. The *MIRAS LC*® is a flexible cooled-wet electrode. The *MIRAS IOC*® is a 6 mm diameter flexible cooled-wet electrode for intraoperative use.

RESULTS (TABLE 2)

Many descriptions of RF lesions are limited to the mean transverse diameter. Standard deviation and range of diameter are not always available. Data on length, ellipticity, distortion, completeness, radius and spatial relationship with the electrode tip are rare to non-existent. Data on the most basic parameter (transverse diameter) in the perfused pig liver are available for only 10 of the 28 electrodes that are presently on the market. Values of the same parameters using a Pringle maneuver are available only for two of the 28 electrodes (Table 2(a)–(c)).

With normal blood flow, diameter or length of RF lesions in pig liver are often smaller and more variable than the length of the electrode tip or the diameter of the deployed prongs suggests (Fig. 3). Radiofrequency lesions rarely are perfect spheres. More often, they are ellipses or flattened spheres (Fig. 3(a) and (b)).

In the perfused liver, type 1 distortion of the RF lesion by nearby blood vessels is very common for all electrodes.[3,5,7,9,12,14,18,22,29,30,33–36] A type 2 distortion is mainly seen with wet electrodes.[41] Incomplete fusion of RF lesions between prongs is noted for both RITA®[5,7,30,31,34,36] and Radiotherapeutics®[13,15] expandable electrodes.

Compared to RF in perfused liver, thermal diameter is larger when performing RF during partial or total blood flow interruption in pig liver and in patients with hepatocellular carcinoma or colorectal metastases. Standard deviation of RF lesion diameter is equal or larger with reduced blood flow. Ellipticity is equal or less with flow reduction. Distortion is less frequent and completeness of fusion is more frequent with hepatic vessel occlusion. All these findings are more pronounced in case of complete interruption of inflow (Pringle maneuver) or outflow (occlusion of hepatic veins), as compared to partial occlusion, i.e. only the hepatic artery or the portal vein.[5,7,10,22,23,31,32,34]

Table 2(a) Description of RF lesions by Radionics® Cool-tip RF® electrodes

Electrode	Blood flow interruption	Mode	Duration (min)	Algorithm deviation	Tissue	Diameter ± SD (range)(cm)	Length ± SD (range)(cm)	Reference
Single 2 cm	no	pulsed	12		pig	2.9 ± 0.3		[8]
Single 3 cm	no	cont	12		pig	2.4 ± 0.2 (2.2–2.8)	(3.3–4.4)	[8,21,22]
	no	cont	12		crm	2.5 ± 0.8 (1.8–3.2)		[22]
	no	cont	10–20	a	crm	2.7 ± 0.9 (1.2–4.4)		[23]
	no	cont	10–20	a	hcc	1.1 ± 0.4 (0.8–1.4)		[23]
	no	cont	12–25		met	2.8 ± 0.3 (2.5–3.1)	3.4 ± 0.3	[24]
	no	cont	30		pig	2.4 ± 0.2	(3.3–4.4)	[22]
	no	pulsed	12		pig	3.7 ± 0.6		[8,25]
	no	pulsed	8–12		hcc & met	3.1 ± 0.4		[26]
	no	pulsed	15		crm	2.5 ± 0.8 (1.4–3.4)		[27]
	no	pulsed	15		hcc	2.9 ± 0.9 (2.6–4.6)		[27]
	hepatic artery	cont	12		pig	2.5 ± 0.1	(3.3–4.4)	[22]
	celiac artery	cont	12		pig	2.7 ± 0.2	(3.3–4.4)	[22]
	portal vein	cont	12		pig	2.9 ± 0.1	(3.3–4.4)	[22]
	portal vein	cont	30		pig	3.2 ± 0.6	(3.3–4.4)	[22]
	full Pringle	cont	12		crm	4.0 ± 1.3 (2.5–5.0)		[22]
	full Pringle	cont	14		met	3.8		[28]
	full Pringle	cont	10–20	a	hcc	3.6		[23]
	full Pringle	cont	10–20	a	crm	3.9 ± 0.1		[23]
Cluster	no	cont	12		pig	3.3 ± 0.2		[29]
	no	cont	10–20		crm	5.5		[23]
	no	cont	20		pig	3.0 ± 0.2		[29]
	no	pulsed	12		pig	4.0 ± 0.1		[8]
	no	pulsed	15		pig	3.4 ± 0.4	4.0 ± 0.5	[30]
	no	pulsed	12–15		crm	5.3 ± 0.6 (4.2–7.0)		[29]

cont, continuous; crm, colorectal metastases; hcc, hepatocellular carcinoma; met, metastases; a = 2.5 or 3 cm tip, grey shaded data are graphically represented in Figure 3.

Table 2(b) Description of RF lesions by RITA Medical Systems® electrodes

Electrode	Blood flow interruption	Temperature	Duration (min)	Algorithm deviation	Tissue	Diameter ± SD (range)(cm)	Length ± SD (range)(cm)	Reference
model 30	no	70	5		pig	(1.2–3.2)	2.3 (1.8–3.0)	[31]
	no	70	7.5		pig	(0.7–3.3)	2.8 (2.0–4.5)	[31]
	no	70	10		pig	(1.3–3.0)	2.7 (1.8–3.5)	[31]
	no	70	10		pig	2.2 (0.4–3.6)	3.1 (2.5–3.5)	[31]
	no	70	12.5		pig	(1.5–3.5)	2.6 (2.1–3.7)	[31]
	no	70	15		pig	(1.2–3.1)	3.1 (2.4–3.7)	[31]
	no	70	20		pig	(1.2–3.1)	3.1 (2.2–4.5)	[31]
	no	80–110	10		hcc	2.2 ± 0.4 (1.6–3.2)		[32]
	no	95	12		pig	max 2.3		[33]
	no	95	13		pig	3 ± 0.9		[4]
	no	95	15		pig	2.9 ± 0.4 (2.0-3.2)	2.6 ± 0.4	[30]
	no	95–115	20		pig	3.0 ± 0.2		[34]
	no	100	6		pig			[35]
	no	100	7		pig	(1.0–2.6)		[7]
	no	100	8		pig	2.6 ± 0.4		[36]
	no	100	8		pig	2.5 ± 0.3		[5]
	no	100	8		pig	2.5 ± 0.3		[37]
	hepatic artery	80–110	10		hcc	3.2 ± 0.7 (2.0–4.2)		[32]
	hepatic artery	95–115	20		pig	3 ± 0.4		[34]
	hepatic artery	100	7		pig	(1.9–3.2)		[7]
	portal vein	95–115	20		pig	3.5 ± 0.3		[34]
	portal vein	100	7		pig	(2.4–3.3)		[7]
	hepatic veins	95–115	20		pig	4 ± 0.3		[34]
	full Pringle	70	10		pig	3.8 (2.7–5.5)	4.8 (3.5–5.5)	[31]
	full Pringle	95–115	20		pig	4 ± 0.2		[34]
	full Pringle	100	8		pig	3.5 ± 0.3		[5]
	full Pringle	100	7		pig	(2.9–3.3)		[7]
StarBurst®	no	100	10	b	pig	2.0 ± 0.4	3.8 ± 1.4	[38]
StarBurstXL®	no	/		b	hcc and met	2.5 ± 0 (2.5–2.5)		[9]
	no	/		c	hcc and met	3.6 ± 0.8 (1.8-5.2)		[9]
	no	/		d	hcc and met	4.2 ± 0.8 (2.6–5.8)		[9]
	no	/		e	hcc and met	5.3 ± 0.6 (3.6-6.5)		[9]
	no	/	18 (17–20)	e	pig	1.5 (1.0–2.0)	4.9 (4.5–5.0)	[10]
	full Pringle	/	18 (17-20)	e	pig	2.8 (1.5–4.0)	5	[10]
	hepatic veins	/	18 (17–20)	e	pig	2.4 (2.0–3.0)	5	[10]
	Pringle + hepatic veins	/	18 (17–20)	e	pig	3.3 (2.0–4.0)	4.9 (4.0–5.3)	[10]

hcc, hepatocellular carcinoma; met, metastases; /, not applicable; b = 2.5 cm deployment, c = 3 cm deployment, d = 4 cm deployment, e = 5 cm deployment, grey shaded data are graphically represented in Figure 3.

Table 2(c) Description of RF lesions by Radiotherapeutics®, Berchtold® and Invatec® electrodes

Electrode	Blood flow interruption	Duration (min)	Algorithm deviation	Tissue	Diameter ± SD (range)(cm)	Length ± SD (range)(cm)	Reference
Radiotherapeutics® LeVeen® 2 cm	no	/		pig	2.4 ± 0.3 (2.0–3.2)	2.0 ± 0.4 (1.2–2.7)	[12]
	no	/		pig	2.8 ± 0.2	2.1 ± 0.1	[14]
	no	/	f	pig	2.9	2.4	[3]
	TAE	/		pig	2.9 ± 0.4 (2.5–3.6)	2.4 ± 0.4 (1.8–2.9)	[12]
Radiotherapeutics® LeVeen® 3 cm	no	/	g	hcc	1.9 ± 0.6 (1–2.8)		[15]
	no	/		hcc	2.2 (0.0–4.2)		[13]
	no	/	h	hcc	2.6 (1.5–3.7)		[13]
Radiotherapeutics® LeVeen® 3.5 cm	no	/		pig	4.1 ± 0.3	3.5 ± 0.2	[14]
	no	/		hcc and met	2.8 ± 0.9 (0.0–4.0)		[17]
Radiotherapeutics® LeVeen® 4 cm	no	/		pig	3.8	3.3	[18]
	no	/		hcc and met	3.9 ± 0.5 (2.0–4.5)		[18]
Berchtold® HiTT® 1.5 cm, 2 mm tip	no	5	i	pig	1.7 ± 0.4 (1.0–2.2)	3.0 ± 0.8 (1.8–4.2)	[39]
	no	6.9 ± 2.3		hcc and met	2.7 (1.6–4.5)		[40]

hcc, hepatocellular carcinoma; met, metastases; /, not applicable; f, variable power increase after initial power of 30 W; g, 3 or 3.5 cm electrodes; starting power 50 W; h, stepwise hook extension; i, only 5 min; power unspecified, grey shaded data are graphically represented in Figure 3.

DISCUSSION

In RFC of liver tumours, precise tailoring of the size and the shape of the thermal lesion is important. The coagulated area should be large enough to encompass both the tumour and a safety margin of 1 cm at all sides. As online ultrasound monitoring of the coagulation zone is unreliable,[3–6] exact prior knowledge of size and shape of a single-session RF lesion and its relation to the electrode tip is essential. A systematical description of these data has not previously been available.

The presented data have to be interpreted with caution. Firstly, they are valid only for the treatment algorithm that has been used and for the tissue in which they have been obtained. It is at present unclear, whether, measurements in the pig liver predict coagulation in human tumours.[42] The one study comparing the RF diameter obtained in pig liver and in patients by the same protocol, found that the mean RF diameter was the same, but that variability was larger in human liver.[22] A second caution is that, data may not be entirely comparable between electrodes and protocols as the method of determining coagulation size varied: macroscopic, microscopic by hematoxylin and eosin staining, microscopic by mitochondrial enzyme staining, or by imaging (CT or MRI). Further, the time lapse between the RF coagulation and the measurement varied between reports. Lastly, in some reports the definitions of transverse diameter and length were somewhat different from ours.

Volume measurements

During the study, a trend to reduce the three-dimensional measurements of the RF lesion to one single value appeared. In some studies, only the calculated volume is reported. This leaves the reader ignorant about the shape of the lesion. Volumetry may be useful in the laboratory to optimise energy deposition, but is useless to the clinician.

Diameter and variability

In some papers, only the maximal diameter is reported. The maximal diameter is important to prevent complications by too large coagulations,[1] but is oncologically irrelevant. Knowledge of the minimal diameter is essential to be sure to cover the tumour and a margin of 1 cm at all sides. Other reports do not mention standard deviation or range, both of which give useful information. Range describes the extreme values, while the mean value ± 2 standard deviations includes 95% of lesions in a Gaussian distribution. Some papers confuse the reader by describing the standard error of the mean instead of the standard deviation. The use of standard error of the mean in this context is statistically inappropriate and gives a false impression of high reproducibility.

Radius

Knowledge of the radius would be more useful than knowledge of diameter. However, no data on minimal and maximal radius of RF lesions was found for any electrode. For symmetrical lesions, the radius refers to half of the transverse diameter. Thermal lesions, however, may be asymmetrical in up to 60%.[5]

Size and shape

With normal blood flow, the size of RF lesions is often smaller and more variable than suggested by the length of the electrode tip or the diameter of the deployed prongs. The use of e.g. a '3-cm' electrode does not guarantee a 3 cm minimal coagulation.

RF lesions are rarely perfectly spherical. Their shape is usually closer to an ellipse or a flattened sphere. The likely shape of the thermal lesion should be carefully taken into account when planning the coagulation.

Spatial relation with electrode tip

There are at present no data available to the physician as to the spatial relation between the coagulation lesion and the position of the tip of the electrode. A recent paper suggests an excentric coagulation for the RITA® model 70 and StarBurst XL® electrodes, in contrast to a concentric coagulation for the RITA® model 30 electrode.[9] The spatial location of the coagulation zone for the MIRAS RC® and MIRAS LN® electrodes is not obvious at first glance.

Effect of blood flow

Several studies conclude that complete blood flow interruption by a Pringle maneuver or by hepatic vein occlusion, yields RF lesions that are larger, less elliptic, less distorted, and more completely fused, than are coagulations in a perfused liver. This may in part explain the trend toward less local recurrence (4–9%[43,44]) in series using a Pringle maneuver than using a percutaneous approach (30–60%[2,29,45,46]).

When RF was first introduced in 1992,[3] it was entirely experimental and considered as a *palliative* treatment. The percutaneous route in that context was justified as the least invasive and less costly approach. While formal proof of the therapeutic value of RF awaits the results of randomised trials such as the recently opened EORTC CLOCC 4004 trial, there are at present good indications that RF may be a potentially *curative* treatment. If cure is possible, then the *most reliable* treatment protocol should be chosen, even if it is more invasive and costly. At this moment, the most reliable coagulations in animal experiments are obtained by a surgical (open or laparoscopic) approach with a Pringle maneuver and by

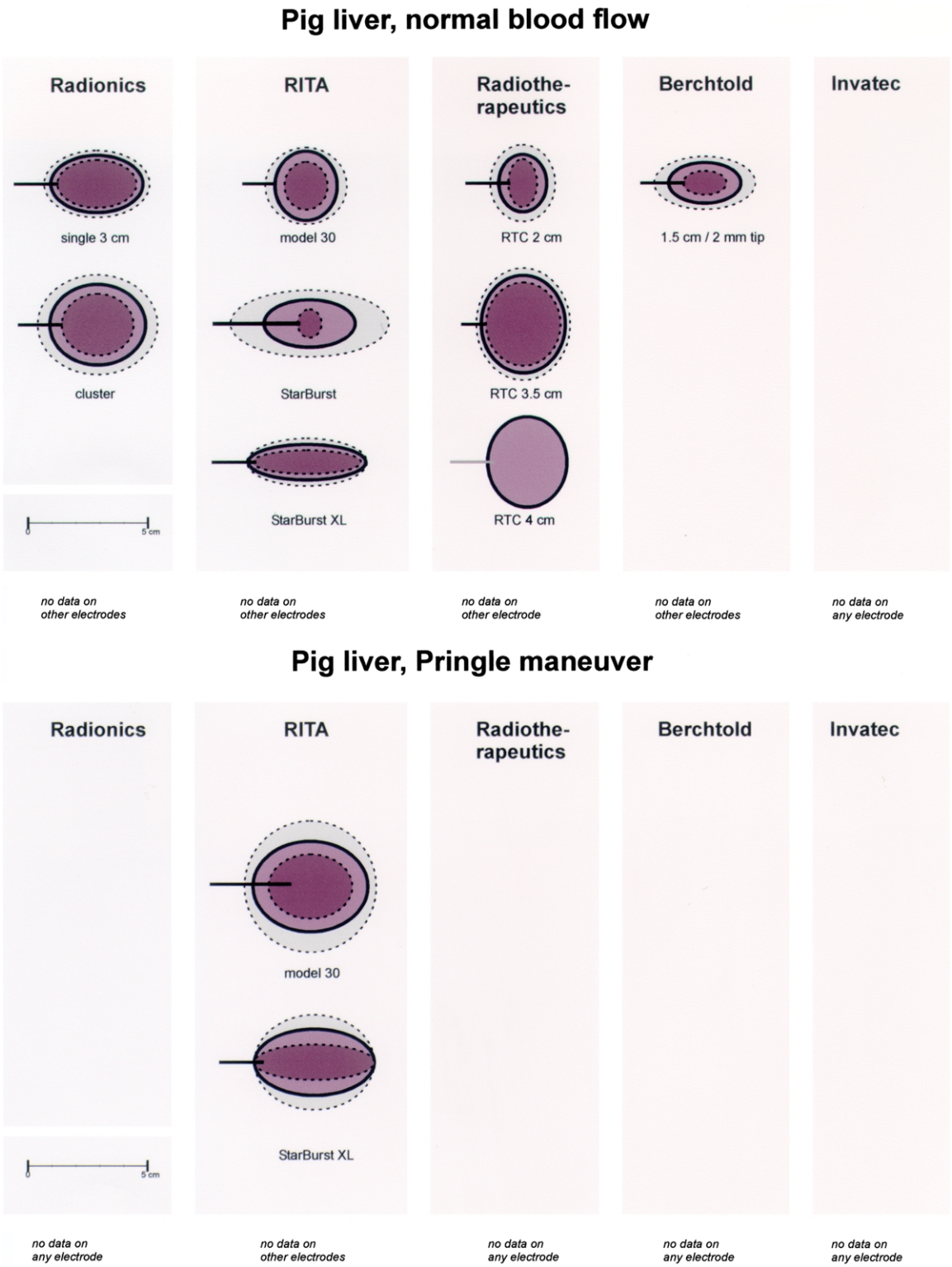

Figure 3 (a) Size and geometry in pig liver with normal blood flow. Pictures are a graphical representation of the grey shaded data from Table 2. Dark coloured = minimal dimensions; medium coloured = mean dimensions; light coloured = maximal dimensions. Minimal and maximal dimensions are based on range when available; if not they were estimated by calculating the mean ± 2 standard deviations which in a Gaussian distribution encompasses 95% of observations. (b) Size and geometry in pig liver with Pringle maneuver. Pictures are a graphical representation of the grey shaded data from Table 2. Dark coloured = minimal dimensions; medium coloured = mean dimensions; light coloured = maximal dimensions.

a percutaneous approach with balloon occlusion of one hepatic vein.[47]

CONCLUSIONS

Few data are available today on basic performances of commercial electrodes. This paucity of data is worrying, given the rapid pace of spread of RF among physicians dealing with liver tumours. In the authors' view, exposing patients to treatments with new electrodes in the absence of animal experimental data is frightening and ethically debatable, even if these electrodes are EU- or FDA-approved. The authors strongly recommend that new electrodes be not approved for release on the market without a complete set of experimental data on the size and geometry of the coagulation lesions in perfused pig liver with and without Pringle maneuver. Companies should also quickly provide data for those electrodes that are already for sale.[48] Better knowledge will hopefully lead to better local tumour control.

ACKNOWLEDGEMENTS

The authors wish to thank Marie-Bernadette Jacqmain for the illustrations and Christian Deneffe for lay-out.

REFERENCES

1. Mulier S, Mulier P, Ni Y *et al.* Complications of radiofrequency coagulation of liver tumours. *Br J Surg* 2002; **89**: 1206–22.
2. Kuvshinoff BW, Ota DM. Radiofrequency ablation of liver tumors: influence of technique and tumor size. *Surgery* 2002; **132**: 605–11.
3. Raman SS, Lu DSK, Vodopich DJ *et al.* Creation of radiofrequency lesions in a porcine model: correlation with sonography, CT and histopathology. *AJR* 2000; **175**: 1253–8.
4. Cha CH, Lee FT, Gurney JM *et al.* CT versus sonography for monitoring radiofrequency ablation in a porcine liver. *AJR* 2000; **175**: 705–11.
5. Scott DJ, Fleming JB, Watumull LM *et al.* The effect of hepatic inflow occlusion on laparoscopic radiofrequency ablation using simulated tumors. *Surg Endosc* 2002; **16**: 1286–91.
6. Leyendecker JR, Dodd GD III, Halff GA *et al.* Sonographically observed echogenic response during intraoperative radiofrequency ablation of cirrhotic livers: pathologic correlation. *AJR* 2002; **178**: 1147–51.
7. Chinn SB, Lee FT Jr., Kennedy GD *et al.* Effect of vascular occlusion on radiofrequency ablation of the liver: results in a porcine model. *AJR* 2001; **176**: 789–95.
8. Goldberg SN, Stein MC, Gazelle GS *et al.* Percutaneous radiofrequency tissue ablation: optimization of pulsed radiofrequency technique to increase coagulation necrosis. *JVIR* 1999; **10**: 907–16.
9. Berber E, Flesher NL, Siperstein AE. Initial clinical evaluation of the RITA 5-centimeter radiofrequency thermal ablation catheter in the treatment of liver tumors. *Cancer J* 2000; **6**(Suppl. 4): S319–29.
10. Chang CK, Hendy MP, Smith JM *et al.* Radiofrequency ablation of the porcine liver with complete hepatic vascular occlusion. *Ann Surg Oncol* 2002; **9**: 594–8.
11. RITA® product information, 2002.
12. Sugimori K, Morimoto M, Shirato K *et al.* Radiofrequency ablation in a pig liver model: effect of transcatheter arterial embolization on coagulation diameter and histologic characteristics. *Hepatol Res* 2002; **24**: 164–73.
13. Kobayashi M, Ikeda K, Someya T *et al.* Stepwise hook extension technique for radiofrequency ablation therapy of hepatocellular carcinoma. *Oncology* 2002; **63**: 139–44.
14. Horigome H, Nomura T, Saso K *et al.* Percutaneous radiofrequency ablation therapy using a clustered electrode in the animal liver. *Hepatogastroenterology* 2001; **48**: 163–5.
15. Morimoto M, Sugimori K, Shirato K *et al.* Treatment of hepatocellular carcinoma with radiofrequency ablation: radiologic–histologic correlation during follow-up periods. *Hepatology* 2002; **35**: 1467–75.
16. Curley SA, Izzo F, Delrio P *et al.* Radiofrequency ablation of unresectable primary and metastatic hepatic malignancies. Results in 123 patients. *Ann Surg* 1999; **230**: 1–8.
17. Lawson TT. Radiofrequency induced necrosis in soft tissues. A review of deployment in animals and humans. Unpublished article provided by Radiotherapeutics®, 2000.
18. Curley SA, Izzo F. Radiofrequency ablation of malignant liver tumors. Unpublished article provided by Radiotherapeutics®, 2001.
19. Anonymous. Physician information. Available at http://www.berchtold.de/e_arzt.htm. Accessed, 31-12-2002.
20. Invatec® product information, 2002.
21. Goldberg SN, Gazelle GS, Solbiati L *et al.* Radiofrequency tissue ablation: increased lesion diameter with a perfusion electrode. *Acad Radiol* 1996; **3**: 636–44.
22. Goldberg SN, Hahn PF, Tanabe KK *et al.* Percutaneous radiofrequency tissue ablation: does perfusion-mediated tissue cooling limit coagulation necrosis? *JVIR* 1998; **9**: 101–11.
23. Goldberg SN, Gazelle GS, Compton CC *et al.* Treatment of intrahepatic malignancy with radiofrequency ablation. Radiologic-pathologic correlation. *Cancer* 2000; **88**: 2452–63.
24. Solbiati L, Goldberg SN, Ierace T *et al.* Hepatic metastases: percutaneous radio-frequency ablation with cooled-tip electrodes. *Radiology* 1997; **205**: 367–73.
25. Goldberg SN, Ahmed M, Gazelle GS *et al.* Radio-frequency thermal ablation with NaCl solution injection: effect of electrical conductivity on tissue heating and coagulation—phantom and porcine liver study. *Radiology* 2001; **219**: 157–65.
26. Solbiati L, Goldberg SN, Livraghi T *et al.* Radiofrequency thermal ablation: increased treatment effect with saline pre-treatment. *Radiology* 2000; **217**(Suppl.): P607.
27. Kelekis AD, Terraz S, Roggan A *et al.* Percutaneous treatment of liver tumors with an adapted probe for cooled-tip, impedance-controlled radio-frequency ablation under open-magnet MR guidance: initial results. *Eur Radiol* 2003; **13**: 1100–5.
28. Elias D, Debaere T, Mutillo I *et al.* Intraoperative use of radiofrequency treatment allows an increase in the rate of curative liver resection. *J Surg Oncol* 1998; **67**: 190–1.
29. Goldberg SN, Solbiati L, Hahn PF *et al.* Large-volume tissue ablation with radio frequency by using a clustered, internally cooled electrode technique: laboratory and clinical experience in liver metastases. *Radiology* 1998; **209**: 371–9.
30. de Baere T, Denys A, Johns Wood B *et al.* Radiofrequency liver ablation: experimental comparative study of water-cooled versus expandable systems. *AJR* 2001; **176**: 187–92.
31. Patterson EJ, Scudamore CH, Owen DA *et al.* Radiofrequency ablation of porcine liver *in vivo*. Effects of blood flow and treatment time on lesion size. *Ann Surg* 1998; **227**: 559–65.
32. Yamasaki T, Kurokawa F, Shirahashi H *et al.* Percutaneous radiofrequency ablation therapy for patients with hepatocellular carcinoma during occlusion of hepatic blood flow. Comparison with standard percutaneous radiofrequency ablation therapy. *Cancer* 2002; **95**: 2353–60.
33. Lee FT, Staelin ST, Haemmerich D *et al.* Bipolar RF produces larger

zones of necrosis than conventional monopolar RF in pig livers. *Radiology* 2000; **217**: 229.
34. Rossi S, Garbagnati F, De Francesco I *et al.* Relationship between the shape and size of radiofrequency induced thermal lesions and hepatic vascularization. *Tumori* 1999; **85**: 137–41.
35. Hansen PD, Rogers S, Corless CL *et al.* Radiofrequency ablation lesions in a pig liver model. *J Surg Res* 1999; **87**: 114–21.
36. Scott DJ, Young WN, Watumull LM *et al.* Accuracy and effectiveness of laparoscopic vs open hepatic radiofrequency ablation. *Surg Endosc* 2001; **15**: 135–40.
37. Scott DJ, Young WN, Watumull LM *et al.* Development of an *in vivo* tumor mimic model for learning radiofrequency ablation. *J Gastrointest Surg* 2000; **4**: 620–5.
38. Wright AS, Haemmerich DG, Mahvi DM *et al.* Hepatic microwave ablation: radiologic–pathologic correlation and comparison with radiofrequency ablation. *Radiology* 2002; **225**(Suppl.): P637–8.
39. Hänsler J, Neureiter D, Strobel D *et al.* Cellular and vascular reactions in the liver to radio-frequency thermo-ablation with wet needle applicators. Study on juvenile domestic pigs. *Eur Surg Res* 2002; **34**: 357–63.
40. Kettenbach J, Kostler W, Rucklinger E *et al.* Percutaneous saline-enhanced radiofrequency ablation of unresectable hepatic tumors: initial experience in 26 patients. *AJR* 2003; **180**: 1537–45.
41. Miao Y, Ni Y, Mulier S *et al. Ex vivo* experiment on radiofrequency liver ablation with saline infusion through a screw tip cannulated electrode. *J Surg Res* 1997; **71**: 19–24.
42. Denys A, Portier F, Lamarre A *et al.* Hepatic vascular occlusions and radiofrequency liver ablation: from animal experiment to clinical observation? *AJR* 2001; **177**: 1215–6.
43. Curley SA, Izzo F, Ellis LM *et al.* Radiofrequency ablation of hepatocellular cancer in 110 patients with cirrhosis. *Ann Surg* 2000; **232**: 381–91.
44. Curley SA, Izzo F, Delrio P, *et al.* Radiofrequency ablation of malignant liver tumors in 304 patients. Proceedings ASCO, **vol. 19**. Hagerstown, MD: Lippincott Williams and Wilkins, 2000: 248A.
45. Solbiati L, Ierace T, Tonolini M *et al.* Radiofrequency thermal ablation of hepatic metastases. *Eur J Ultrasound* 2001; **13**: 149–58.
46. Kainuma O, Asano T, Aoyama H *et al.* Combined therapy with radiofrequency thermal ablation and intra-arterial infusionü chemotherapy for hepatic metastases from colorectal cancer. *Hepato-Gastroenterology* 1999; **46**: 1071–7.
47. de Baere T, Bessoud B, Dromain C *et al.* Percutaneous radiofrequency ablation of hepatic tumors during temporary venous occlusion. *AJR* 2002; **178**: 53–9.
48. Michel LA, Johnson P. Is surgical mystique a myth and double standard the reality? *J Med Ethics: Med Humanit* 2002; **28**: 66–70.

Accepted for publication 19 September 2003

Current address of Stefaan Mulier :

Stefaan Mulier, MD
Philipslaan 66
3000 Leuven
Belgium
+32 16 35 67 86
+32 498 78 73 57
stefaan.mulier@skynet.be
http://drmulier.com/research.html